Available online at www.sciencedirect.com

ScienceDirect

Ceramics International 40 (2014) 2627–2634

CERAMICS INTERNATIONAL

www.elsevier.com/locate/ceramint

Electrocaloric effect based on the depolarization transition in $(1-x)Bi_{0.5}Na_{0.5}TiO_3$–$xKNbO_3$ lead-free ceramics

Xijie Jiang[a], Laihui Luo[a,*], Baoyin Wang[a], Weiping Li[a], Hongbing Chen[b]

[a]Department of Microelectronic Science and Engineering, Ningbo University, China
[b]Institute of Materials Science & Engineering, Ningbo University, China

Received 13 September 2013; received in revised form 10 October 2013; accepted 15 October 2013
Available online 24 October 2013

Abstract

Lead-free ferroelectric ceramics $(1-x)Bi_{0.5}Na_{0.5}TiO_3-xKNbO_3$ (BNT–xKN) with $x=0.00$, 0.04, 0.06 and 0.08 were synthesized by the conventional solid state reaction method. The effects of the $KNbO_3$ addition on the dielectric behavior, ferroelectric properties, as well as electrocaloric effect of the ferroelectric ceramic BNT–xKN were investigated. The results show that the depolarization temperature decreases with the increment of KN content. A high ECE of 1.73 °C is achieved at 76 °C in BNT–0.06KN. The relation between electrocaloric effect and depolarization transition was discussed. This investigation indicates that the depolarization transition below Curie transition in BNT-based ceramics is a promising approach in ECE technique.

Keywords: Ferroelectric; Electrocaloric effect; Lead-free

1. Introduction

To deal with the environmental problems that we are facing, a large number of efforts have been made in environment-friendly solid-state cooling technologies. One of the promising technologies is the electrocaloric effect (ECE). ECE in ferroelectric materials is a promising cooling solution for micro- and nano-electronic devices which have lots of high-power and high-density heat generating components. As early as 1930, ECE was observed for the first time in ferroelectric material Rochelle salt by Kobeco and Kurtschatov [1]. The temperature change was so small, and the working temperature was so low that the ECE was revisited until 1956 [2]. Subsequently, ECE were investigated in a series of ferroelectric materials, such as $LiNbO_3$, $LiTaO_3$, $Li_2SO_4 \cdot H_2O$, KH_2PO_4 [3]. Recent years, it is reported that a giant ECE – a temperature change (ΔT) of as high as 12 K is achieved in lead-based ferroelectric thin films [4–9]. Thin films may appear attractive because large electric fields may be applied to them, resulting in a sharp increase of ECE in the thin films. Research into bulk materials is also of high importance due to their high cooling capacity [10].

Considering the toxicity of lead-based ferroelectric materials, suitable materials are now being considered as potential alternatives to lead-based materials for specific applications [11–19]. $SrBi_2Ta_2O_9$ (SBT) thin film [14] and $Bi_{0.5}Na_{0.5}TiO_3$–$BaTiO_3$ (BNT–BT) bulk ceramic [15] have been reported to have an ECE of 4.93 and ~0.19 K, respectively. Singh et al. [18] reported that an ECE of 0.46 K was achieved in $0.45BaZr_{0.2}Ti_{0.8}O_3$–$0.55Ba_{0.7}Ca_{0.3}TiO_3$ (0.45BZT–0.55BCT) single crystal near the tetragonal-to-cubic phase transition. Novak et al. also reported an ECE of ~1.2 K by high-resolution electrocaloric measurement was obtained in $BaTiO_3$ single crystals [19]. Considering the relatively low ECE reported in lead-free bulk materials, it is necessary to develop potential lead-free ECE materials.

BNT is considered to be a promising candidate because of its relatively large remnant polarization ($P_r=38$ μC/cm^2) and high T_m ($T_m=320$ °C). BNT ceramic exhibits two dielectric anomalies at T_d and T_m, respectively. It is well realized that the long-range ferroelectric order disappears near $T_d \sim 200$ °C, and a broad diffusive dielectric peak and a maximum dielectric constant is observed at T_m. However, the XRD results indicate that the phase evolution as temperature is not consistent with the dielectric behavior [20]. It is well known that the largest

*Corresponding author. Tel.: +86 574 8760 0953.
E-mail address: llhsic@126.com (L. Luo).

0272-8842/$ - see front matter © 2013 Elsevier Ltd and Techna Group S.r.l. All rights reserved.
http://dx.doi.org/10.1016/j.ceramint.2013.10.066

ECE is achieved at the ferroelectric–paraelectric phase transition. For BNT ceramics, the ferroelectric–paraelectric phase transition happens at high temperature over 500 °C. This characteristic is not suitable for low temperature cooling application. Fortunately, it is reported that the phase transition below Curie transition also contributes to the ECE [21]. The occurrence of depolarization below Curie transition will result in a large change of entropy, which will lead to a large ECE. Furthermore, the depolarization temperature can be modified by introducing the second composition, for example, $BaTiO_3$ [16], $NaNbO_3$ [22], $SrTiO_3$ [23], $K_{0.5}Na_{0.5}NbO_3$ (KNN) [24]. Therefore, one can modify the ECE of BNT-based ceramics by adding the second composition. However, the ECE of BNT-based ceramics is investigated a little. Even worse, an opposite ECE is observed in the BNT-based ceramics [15,25], namely negative ECE. Negative ECE suggests that BNT-based ceramics absorb heats (refrigeration effect) during the processes of field applications. However, other ferroelectric ceramics show refrigeration effect during the processes of field removal.

In the present investigation, to find the relation between ECE and the depolarization transition below Curie transition in BNT-based ceramic, $KNbO_3$ (KN) was adopted to add in BNT to form a binary system of $(1-x)Bi_{0.5}Na_{0.5}TiO_3$–$xKNbO_3$ (BNT–xKN) to modify the depolarization temperature and ECE.

2. Experiment

In this study, analytical-grade powders: Bi_2O_3 (99.9%), Na_2CO_3 (99.8%), TiO_2 (99.8%), K_2CO_3 (99%), Nb_2O_3 (99.9%) were used as the raw materials to synthesize lead-free BNT–xKN (x=0.00, 0.04, 0.06 and 0.08) ferroelectric ceramics. BNT–xKN ceramics were prepared by a conventional solid state reaction technique. After sintering at 1150 °C for 2 h, silver paste was pasted on both sides of the disc samples and then fired at 600 °C in order to form electrodes. The density of the ceramics was calculated by Archimedes method, and specific heat capacity was measured by Laser thermal conductivity technique (LFA 457, Germany). The polarization–electric field (P–E) hysteresis loops were measured by ferroelectric tester RT Premier II with a frequency of 10 Hz. The dielectric constant ε_{33} and dielectric loss tan δ as a function of temperature for the samples were tested by the impedance analyzer Agilent 4294A with frequencies 100 Hz, 1 kHz, 10 kHz, 100 kHz and 1 MHz without bias field. The dielectric measurement was performed during heating process with a rate of 2 °C/min.

3. Results and discussion

To characterize the ferroelectric properties of BNT–xKN (x=0.00, 0.04, 0.06, 0.08) ceramics, P–E hysteresis loops of the ceramics were measured at room temperature, as illustrated in Fig. 1. All the BNT–xKN ceramics exhibit a strong ferroelectric property except x=0.08. The BNT–0.00KN ceramic shows a high coercive field E_c of ~52 kV/cm and remnant polarization P_r of ~41 μC/cm^2. However, with the increment of KN content, both the remnant polarization P_r and coercive field E_c are decreased dramatically. When x increasing to 0.06, the loop shows an E_c of ~26 kV/cm and P_r of ~27 μC/cm^2, respectively. The E_c of BNT–0.06KN is smaller than that of BNT–0.04KN. However, the saturated polarization of BNT–0.06KN ceramic at 70 kV/cm is higher than that of BNT–0.04KN. With x further increasing to 0.08, the P–E loop becomes very flattened and slanted, indicating that excess KN addition weakens the ferroelectricity of the ceramics greatly.

Previous to the calculation of ECE, it is necessary to examine the dielectric behavior of the ceramics as a function of temperature. Fig. 2(a) –(d) shows the temperature dependences of ε_{33} and tan δ for all the poled BNT–xKN (x=0.00, 0.04, 0.06, 0.08) ceramics at 100 Hz, 1 kHz, 10 kHz, 100 kHz, and 1 MHz. From Fig. 2(a) and (b) one clearly see that there are three obvious dielectric anomaly peaks at T_d, T_p and T_m, as marked in the figures. The first dielectric anomaly appears at temperature T_d, and T_d is corresponding to the temperature of the first tan δ peak [26]. Near T_d, lots of interesting results are observed in BNT-based ceramics, such as large electric-field induced strain, constricted P–E loops [27,28]. With the KN concentration increasing to 0.06, it can be seen that T_d anomaly at ~35 °C becomes obscure, as shown in Fig. 3. When x increases to 0.08, T_d is not observed in the curves, as shown in Fig. 2(d). The scientific communities still do not reach a consensus on the exact microstructure of pure BNT ceramics. The traditional and widely accepted view of the BNT structure and phase evolution was proposed by Jones and Thomas [20]: $R3c \overset{523\ K}{\longleftrightarrow} R3c+P4bm \overset{670\ K}{\longleftrightarrow} P4bm \overset{813\ K}{\longleftrightarrow} Pm3m$. Also, there are many other opinions on the structure of the BNT structure. For example, Dorcet et al. [29] demonstrated that the phase of BNT at room temperature was a two-phase mixture with the major phase being rhombohedral along with tetragonal platelets. The inconsistency on the reported phase structure of BNT ceramic may be caused by that the phase structure of the BNT is highly susceptible to thermal, mechanical, and electrical stimuli [30]. Pure unpoled BNT exhibits a strong relaxation property and no obvious T_d peak is observed [31]. However, a very sharp dielectric anomaly is observed at T_d=182 °C and no obvious frequency dependence is observed below T_d, as shown in Fig. 2(a). The previous reports show that the electric

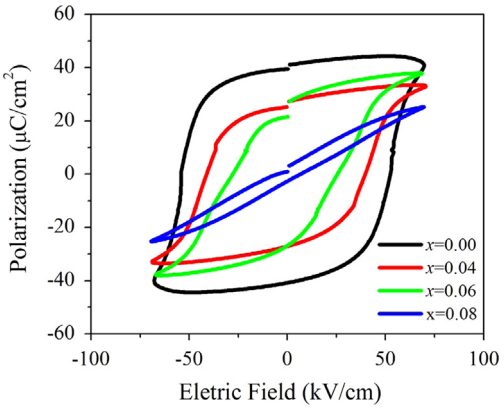

Fig. 1. P–E hysteresis loops of BNT–xKN at room temperature.

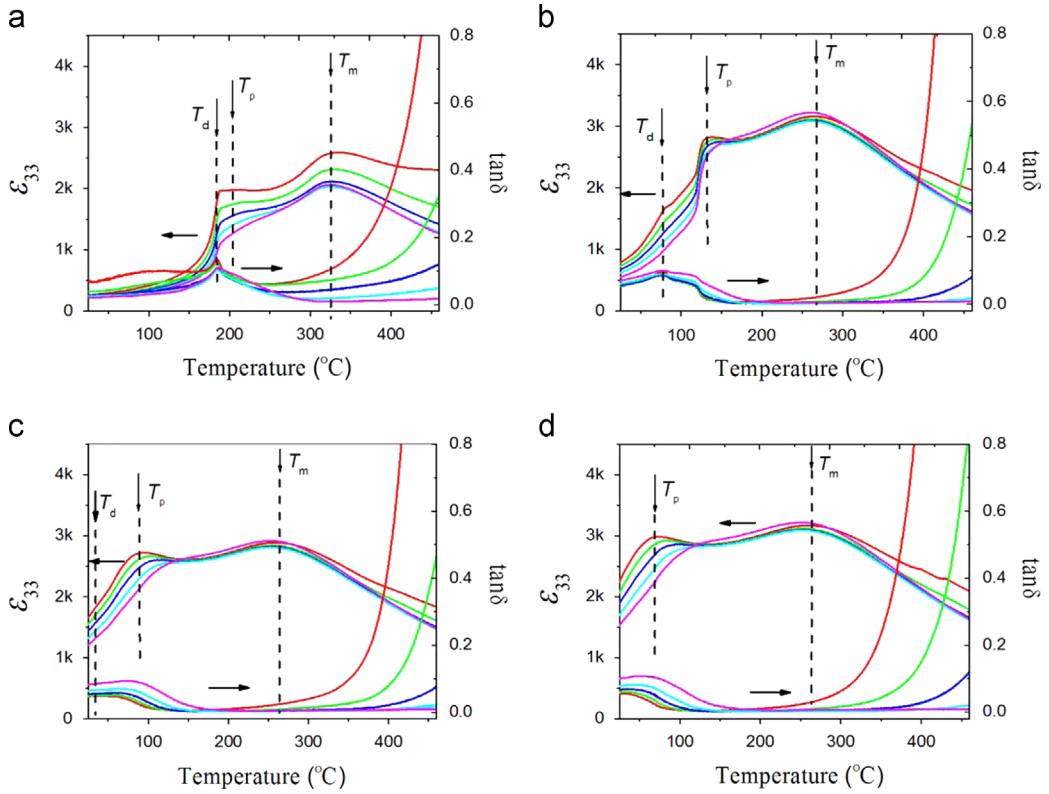

Fig. 2. Temperature dependences of ε_{33} and tan δ for poled BNT–xKN ceramics at 100 Hz, 1 kHz, 10 kHz, 100 kHz and 1 MHz: (a) $x=0$, (b) $x=0.04$, (c) $x=0.06$, (d) $x=0.08$.

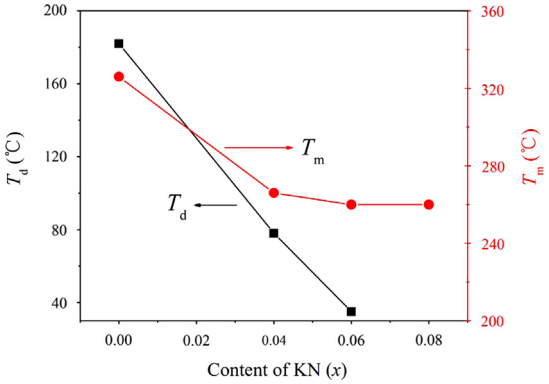

Fig. 3. T_d and T_m as a function of x for the BNT–xKN ceramics.

field can induce long-range ferroelectric order in BNT-based ceramics [31–33]. Na and Bi ions randomly occupy A-sites in the pure BNT ceramics. As a result, relaxation property is observed in the unpoled BNT ceramic [34]. The external electric field can overcome the random field caused by the site-disordering and charge fluctuation. Therefore, long-range ferroelectric order is formed in the poled BNT ceramics, and no obvious relaxation properties are observed below T_d. However, the KN introduction increases the site disordering and charge fluctuation. As a result, T_d decreases with the increment of KN content. Hence, it is reasonable to assume that the long-range ferroelectric order cannot be formed in the BNT ceramic with $x=0.08$ due to the enhanced random field even after poling (Fig. 2(d)). Therefore, it is most possible that the T_d anomaly is caused by the ferroelectric-relaxor transition [33]. The ferroelectric-relaxor phase transition temperature for BNT–0.08KN is lower than the measured temperature range. As a result, T_d peak is not observed in the curves. It should be noted that the depolarization mechanism was always under debate. At first, most of the researchers considered that the depolarization was caused by ferroelectric to anti-ferroelectric phase transition [27,28,35]. Recently, Dorcet et al. [36] proposed that the intermediate orthorhombic phase should response to the depolarization and relaxation behavior above T_d. The second dielectric anomaly peak appears at temperature T_p. It can be seen that T_p is dependent on the measurement frequency, and this dielectric anomaly becomes obscure when the test frequency increases to 1 MHz, as shown in Fig. 2(a)–(d). The relaxation behavior should be responsible for this dielectric anomaly. The third dielectric anomaly appears at temperature T_m, at which ε_{33} reaches the maximum value, see Fig. 2. Compared with that of pure BNT ceramics, T_m of the BNT–xKN ceramics becomes fuzzier with the increment of KN concentration, as shown in Fig. 2(a)–(d).

T_d decreases rapidly with the increase of x, as shown in Fig. 3. When x increases to 0.08, T_d is reduced to a temperature lower than the test temperature, resulting in a weak ferroelectric. These results are consistent with the results in Fig. 1. However, T_m first decreases with x increment, and then varies little.

In order to calculate the ECE of the prepared BNT–xKN ($x=0.00$, 0.04, 0.06, 0.08) ceramics, the P–E loops were

measured from 20 to 150 °C every 10 °C, as shown in Fig. 4 (a)–(d). Fig. 4(a) shows several representative loops at different temperatures for the BNT–0.00KN ceramic. The figure shows that the polarization increases with temperature, meanwhile the E_c decreases with the temperature. The increased polarization with temperature results in an increased depolarization rate as the temperature increases further [21], which will lead to an enhanced ECE. Usually, the polarization of the ferroelectrics decreases with the increment of temperature. However, the present case is contrary to this rule. This abnormal behavior may be caused by the electric-field-induced phase transition from rhombohedral to tetragonal. With the increment of the KN content and this abnormal behavior is not observed in BNT–0.08KN (Fig. 4(d)). Rhombohedral BNT ceramics may transform to pseudocubic phase due to the increased KN content [37]. An obvious constricted *P–E* loop is also observed at 60 °C for the BNT–0.06KN ceramic (Fig. 4(c)). Fig. 5 shows the polarization as a function of temperature under different fields for BNT–*x*KN ceramics. The polarization was extracted from the upper hysteresis loops. The curves were fitted by fourth-order polynomial. Fig. 5(a) shows that the polarization of the BNT–0.00KN ceramic under different electric fields increases with the temperature. However, the polarization of the BNT–0.04KN and BNT–0.06KN ceramics first increases with the temperature and then decreases with further increment of temperature, as shown in Fig. 5(b) and (c), respectively. However, when the KN content increases to $x=0.08$, all the polarization decreases as the temperature increases, which indicates that the external field does not induce a phase transition in the BNT–0.08KN ceramic.

The pyroelectric coefficients $(\partial P/\partial T)_E$ under electric field were calculated from the derivation of the fitted polynomial, as shown in Fig. 6. From Fig. 6 we know that $(\partial P/\partial T)_E$ values are sensitive to both the temperature and electric field. Large $(\partial P/\partial T)_E$ value will result in large ECE. The $(\partial P/\partial T)_E$ value of BNT–0.00KN is positive, as shown in Fig. 6(a). The abnormal positive $(\partial P/\partial T)_E$ value is caused by the increased polarization with temperature, as mentioned above. The positive $(\partial P/\partial T)_E$ value will result in a negative temperature change. In another word, the removal of external field upon BNT–0.00KN will increase, rather decrease, the temperature under adiabatic conditions. For the BNT–0.04KN ceramics, the $(\partial P/\partial T)_E$ value transfers from positive to negative with the temperature increment, as shown in Fig. 6(b). Fig. 6(c) shows the $(\partial P/\partial T)_E$ value of the BNT–0.06KN ceramics as a function of temperature under different bias fields. $(\partial P/\partial T)_E$ value is positive near room temperature, and the value decreases with the bias field increment. Furthermore, the downward $(\partial P/\partial T)_E$ peaks shift toward high temperature as the bias field increases. Pyroelectric coefficient $(\partial P/\partial T)_E$ in Fig. 6(b) and (c) is equivalent to pyroelectric coefficient under bias fields. Pyroelectric coefficient has largest value near depolarization temperature. In other word, the downward pyroelectric coefficient $(\partial P/\partial T)_E$ peak temperature approximately reflects the

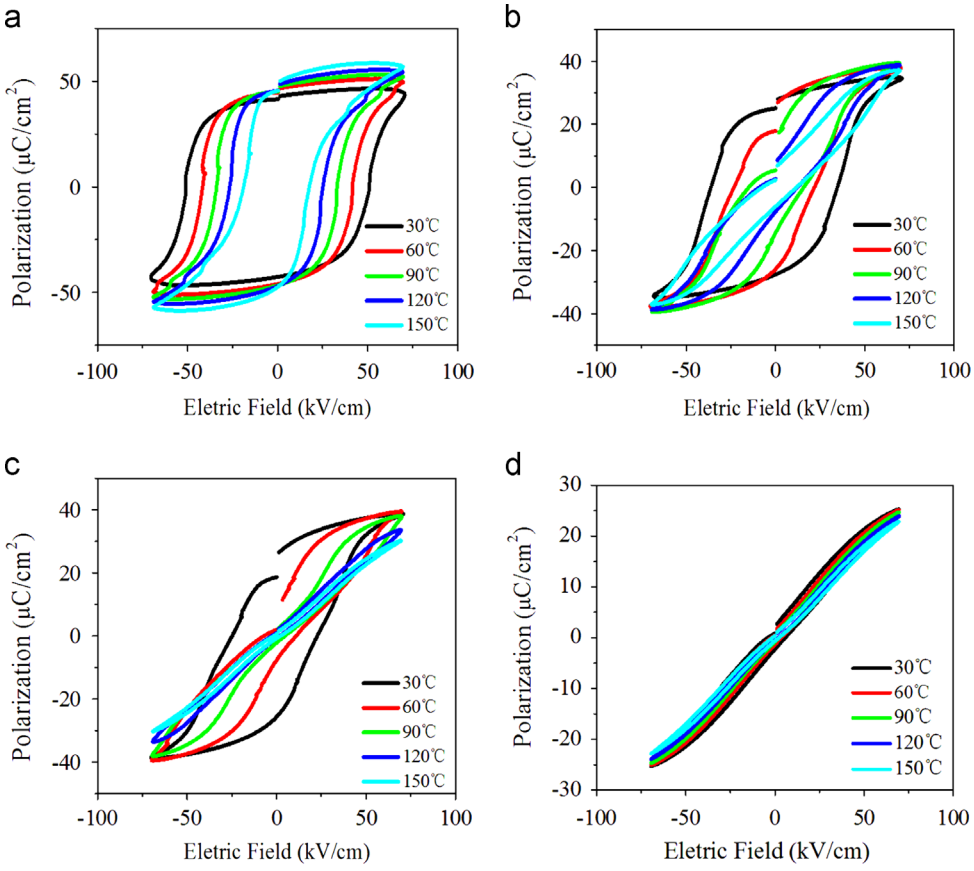

Fig. 4. *P–E* hysteresis loops of the BNT–*x*KN ceramics at several representative temperatures: (a) $x=0$, (b) $x=0.04$, (c) $x=0.06$, (d) $x=0.08$.

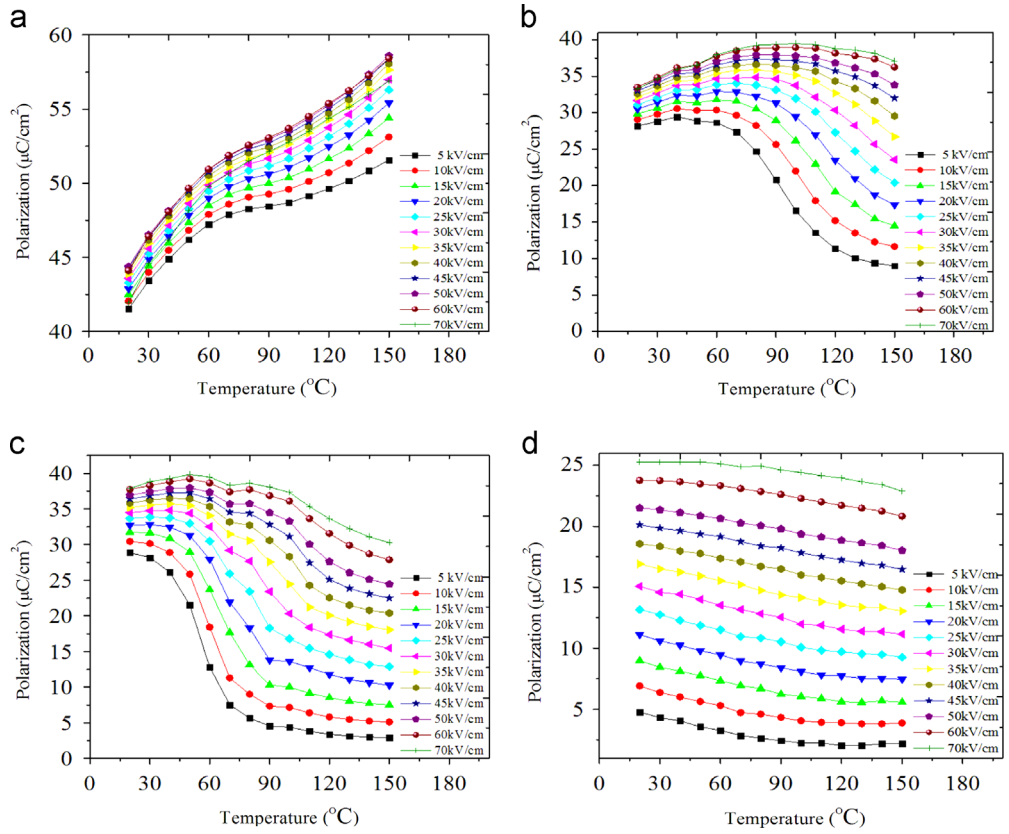

Fig. 5. Polarization as a function of temperature under different electric fields for BNT–xKN ceramics: (a) $x=0$, (b) $x=0.04$, (c) $x=0.06$, (d) $x=0.08$.

depolarization temperature of the ceramics under bias fields. The shift of $(\partial P/\partial T)_E$ peaks toward high temperature with the increment of bias fields in Fig. 6(b) and (c) suggests that bias fields favor the increment of depolarization temperature. The external field favors the long-range ferroelectric order. Hence, the ferroelectric-relaxor transition temperature, namely depolarization temperature, increases with external electric field. Also Ge et al. [38] reported that the depolarization temperature increased with the increment of the bias field. Since the dielectric measurement was performed under no bias field, the temperatures responding to the downward pyroelectric coefficient peak under different bias fields in Fig. 6(b) and (c) are much higher than the depolarization temperatures (Fig. 3) determined by dielectric measurement. The relation between the depolarization temperature and bias fields for BNT–0.00KN and BNT–0.08KN is not mentioned, because the depolarization temperature is not in the temperature range of P–E loop test. When KN content increases to 0.08, $(\partial P/\partial T)_E$ value becomes very small (Fig. 6(d)).

Fig. 7 shows the adiabatic temperature change ΔT under different electric field changes ΔE. The adiabatic temperature change ΔT due to an applied electric field E was calculated according to the following formula [5]: $\Delta T = -(T/\rho C_p)\int_{E_1}^{E_2}(\partial P/\partial T)_E$, where ρ is density of the material and C_p is specific heat capacity. The formula is based on Maxwell relation $(\partial S/\partial E)_T = (\partial P/\partial T)_E$. When calculating ECE, $E_1=0$ kV/cm and $E_2=70$ kV/cm were used. In the temperature range from room temperature to 150 °C, ρ and C_p were taken as constant, as listed in Table 1. Fig. 7(a) shows the ECE of the BNT–0.00KN ceramic. Under all electric field changes, the BNT–0.00KN ceramic shows a converse ECE, namely a negative temperature change. Similar abnormal results were also reported by Bai et al. [15] in the BNT-based ceramics. Also Zheng et al. [25] reported an abnormal ECE of as high as −2.1 °C in BNT–BT ceramics. The negative ECE was also observed in $PbMg_{1/3}Nb_{2/3}O_3$–$PbTiO_3$ single crystal, which was caused by the rhombohedral to tetragonal phase transition [39]. Ponomareva and Lisenov [40] attributed the occurrence of the negative ECE in the ferroelectrics to the application of an electric field in a direction non-colinear to the polar direction of the poled single crystal. Furthermore, the positions of the upward peaks in Fig. 7(a) do not shift under different electric field changes. As KN content x increases to 0.04, the ECE of BNT–0.04KN is positive at high temperature, as shown in Fig. 7(b). Furthermore, ΔT peaks move to high temperature with the increment of field change. The shift of the ECE peaks is ascribed to the shift of depolarization temperature. The samples with $x=0.04$ have a temperature change of 1.33 °C at 125 °C under a change of electric field 70 kV/cm. When x increases to 0.06, a high temperature change of 1.73 °C is observed at 76 °C (Fig. 7(c)). The present results are much higher than the previous reported values [15,18,41]. However, when x increases to 0.08, the ECE of BNT–0.08KN is very small, only a value of 0.23 °C at 70 °C even under 70 kV/cm change.

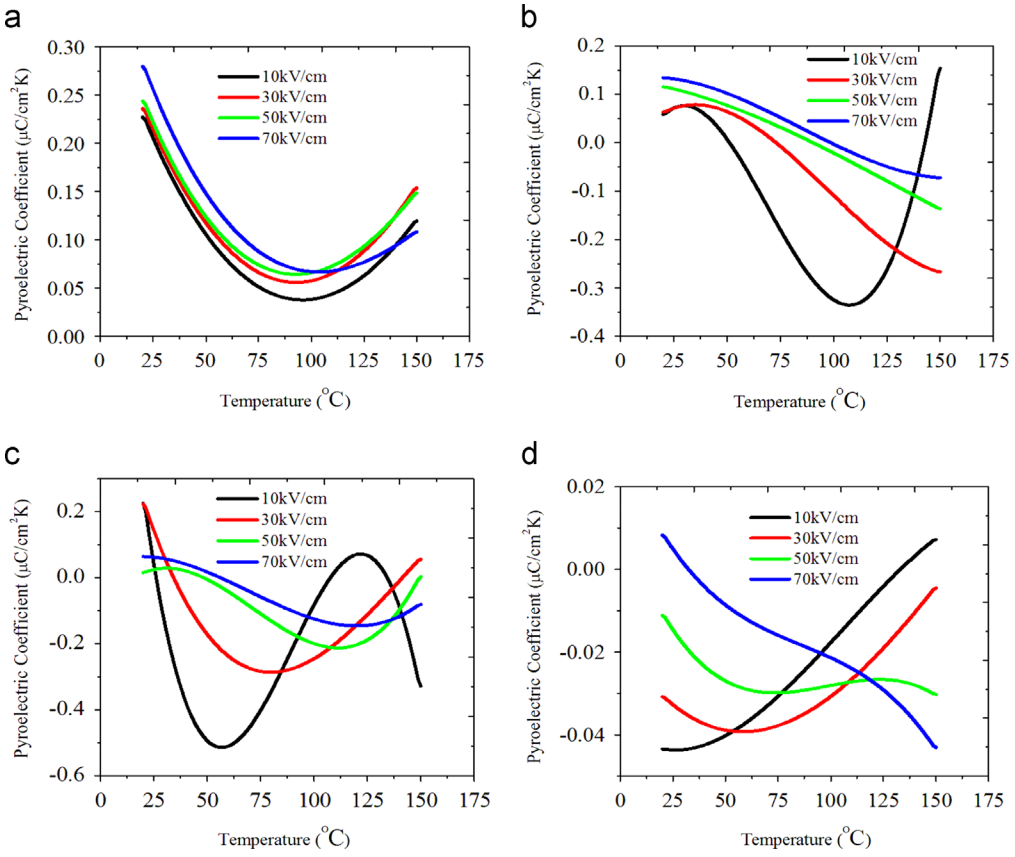

Fig. 6. Pyroelectric coefficient as a function of temperature under different electric fields for BNT–xKN ceramics: (a) x=0, (b) x=0.04, (c) x=0.06, (d) x=0.08.

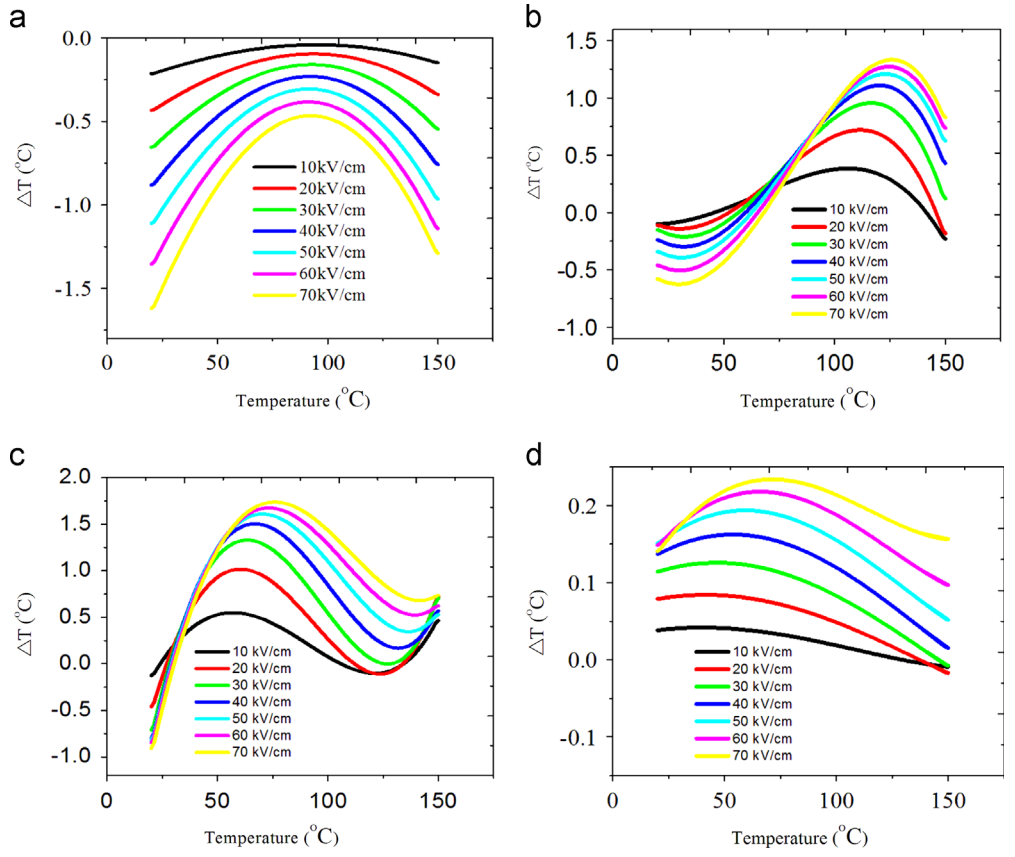

Fig. 7. Adiabatic temperature change ΔT due to different electric field changes for BNT–xKN ceramics: (a) x=0, (b) x=0.04, (c) x=0.06, (d) x=0.08.

Table 1
The permittivity, dielectric loss, depolarization temperature, Curie temperature, density, specific heat capacity, temperature for the maximum ECE and the maximum of temperature change, and the maximum electrocaloric coefficient of BNT–xKN ceramics.

Compositions	ε_{33}	tan δ (%)	T_d (°C)	T_m (°C)	$\rho \times 10^3$ (kg/m^3)	C_p (J/(kg K))	T (°C)	ΔT_{max} (K)	ξ_{max} (K cm/kV)
x=0.00	380	2.5	182	326	5.91	523	20	−1.62	−0.023
x=0.04	750	5.03	78	266	5.86	556	125	1.33	0.019
x=0.06	1606	5.78	35	260	5.67	548	76	1.73	0.025
x=0.08	1977	5.7	–	260	5.53	555	70	0.23	0.003

Table 1 reveals the basic physical properties of BNT–xKN ceramics. The density and heat capacity vary little with the KN content, which indicates that the ECE is mainly dependent on the pyroelectric $(\partial P/\partial T)_E$ value. Electrocaloric coefficient is calculated according to $\xi_{max} = \Delta T_{max}/\Delta E_{max}$, where ΔT_{max} is the maximum temperature change, and ΔE_{max} is the corresponding largest electric field change. A maximum electrocaloric coefficient of 0.025 K cm/kV is achieved in BNT–0.06KN ceramic, which is significantly higher than other lead-free ferroelectric, such as BNT–BT (ξ_{max}=0.005 K cm/kV) [15] and SBT (ξ_{max}=0.008 K cm/kV) [14].

4. Conclusions

In conclusion, the ECE of BNT–xKN ceramics have been investigated. The results demonstrate that the ECE of the ceramics is concerned with the depolarization behavior. BNT–0.00KN ceramics have a negative ECE in the measured temperature range. With the increment of KN content, the depolarization temperature shifts to low temperature. Consequently, the ECE of BNT–0.04KN and BNT–0.06KN ceramics transits from negative at low temperature to positive at high temperature. Furthermore, the ECE peaks shift to high temperature with external field due to the increased depolarization temperature. A high ECE of 1.73 °C is achieved at 76 °C in BNT–0.06KN. The present investigation demonstrates that the depolarization transition below Curie transition in BNT-based ceramics is a promising approach in ECE technique.

Acknowledgments

This work was supported by the National Natural Science Foundation of China (Nos. 51002082 and 61378068), Natural Science Foundation of Ningbo (2012A610118), and the K. C. Wong Magna Fund in Ningbo University (xkzl1203).

References

[1] P. Kobeco, I.V. Kurtchatov, Dielectric properties of Rochelle salt crystal, Z. Phys. 66 (1930) 192–205.
[2] H. Grnicher, Induzierte Ferroelektrizitat von $SrTiO_3$ bei sehr tiefen Temperatur und uber dieKalterzeugung durch adiabatic Entpolarisierung, HeIvetica Phys. Acta 29 (1956) 210–212.
[3] R. Radebaugh, W.N. Lawless, J.D. Siegwarth, A.J. Morrow, Feasibility of electrocaloric refrigeration for the 4–15 deg K temperature range, Cryogenics 19 (1979) 187–208.
[4] A.S. Mischenko, Q. Zhang, J.F. Scott, R.W. Whatmore, N.D. Mathur, Giant electrocaloric effect in thin-film $PbZr_{0.95}Ti_{0.05}O_3$, Science 311 (2006) 1270–1271.
[5] B. Neese, S.G. Lu, B. Chu, Q.M. Zhang, Electrocaloric effect of the relaxor ferroelectric poly (vinylidene fluoride-trifluoroethylene-chlorofluoroethylene) terpolymer, Appl. Phys. Lett. 94 (2009) 042910–042913.
[6] S.G. Lu, B. Rozic, Q.M. Zhang, Z. Kutnjak, X. Li, E. Furman L.J. Gorny, M. Lin, B. Malic, M. Kosec, R. Blinc, R. Pirc, Organic and inorganic relaxor ferroelectrics with giant electrocaloric effect, Appl. Phys. Lett. 97 (2010) (162904-3).
[7] T.M. Correia, J.S. Young, R.W. Whatmore, J.F. Scott, N.D. Mathur, Q. Zhang, Investigation of the electrocaloric effect in a $PbMg_{2/3}Nb_{1/3}O_3$–$PbTiO_3$ relaxor thin film, Appl. Phys. Lett. 95 (2009) (182904-3).
[8] J. Parui, S.B. Krupanidhi, Electrocaloric effect in antiferroelectric PbZrO3 thin films, Phys. Status Solidi 2 (2008) 230–232.
[9] J. Karthik, L.W. Martin, Effect of domain walls on the electrocaloric properties of $Pb(Zr_{1-x},Ti_x)O_3$ thin films, Appl. Phys. Lett. 99 (2011) (032904-3).
[10] M. Valant, Electrocaloric materials for future solid-state refrigeration technologies, Prog. Mater. Sci. 57 (2012) 980–1009.
[11] G. Akcay, S.P. Alpay, J.V. Mantese, G.A. Rossetti, Magnitude of the intrinsic electrocaloric effect in ferroelectric perovskite thin films at high electric fields, Appl. Phys. Lett. 90 (2007) 252909 (3 pp.).
[12] G. Akcay, S.P. Alpay, G.A. Rossetti, J.F. Scott, Influence of mechanical boundary conditions on the electrocaloric properties of ferroelectric thin films, J. Appl. Phys. 103 (2008) 024104–024107.
[13] H.X. Cao, Z.Y. Li, Electrocaloric effect in $BaTiO_3$ thin films, J. Appl. Phys. 106 (2009) 094104–094105.
[14] H. Chen, T. Ren, X. Wu, Y. Yi, L. Liu, Giant electrocaloric effect in lead-free thin film of strontium bismuth tantalite, Appl. Phys. Lett. 94 (2009) 182902–182903.
[15] Y. Bai, G.P. Zheng, S.Q. Shi, Abnormal electrocaloric effect of $Na_{0.5}Bi_{0.5}TiO_3$–$BaTiO_3$ lead-free ferroelectric ceramics above room temperature, Mater. Res. Bull. 46 (2011) 1866–1869.
[16] Y. Bai, G.P. Zheng, S.Q. Shi, Kinetic electrocaloric effect and giant net cooling of lead-free ferroelectric refrigerants, J. Appl. Phys. 108 (2010) 104102–104104.
[17] J. Zhang, I.B. Misirlioglu, S.P. Alpay, G.A. Rossetti, Electrocaloric properties of epitaxial strontium titanate films, Appl. Phys. Lett. 100 (2012) (222909-4).
[18] G. Singh, I. Bhaumik, S. Ganesamoorthy, R. Bhatt, A.K. Karnal, V.S. Tiwari, P.K. Gupta, Electro-caloric effect in $0.45BaZr_{0.2}Ti_{0.8}O_3$–$0.55Ba_{0.7}Ca_{0.3}TiO_3$ single crystal, Appl. Phys. Lett. 102 (2013) 082902–082904.
[19] N. Novak, Z. Kutnjak, R. Pirc, High-resolution electrocaloric and heat capacity measurements in barium titanate, Europhys. Lett. 103 (2013) 47001 (-p5).
[20] G.O. Jones, P.A. Thomas, Investigation of the structure and phase transitions in the novel A-site substituted distorted perovskite compound $Na_{0.5}Bi_{0.5}TiO_3$, Acta Crystallogr. Sec. B 58 (2002) 168–178.
[21] L. Luo, M. Dietze, C. Solterbeck, M. Es-Souni, H. Luo, Orientation and phase transition dependence of the electrocaloric effect in $0.71PbMg_{1/3}Nb_{2/3}O_3$–$0.29PbTiO_3$ single crystal, Appl. Phys. Lett. 101 (2012) (062907-4).
[22] Y.M. Li, W. Chen, J. Zhou, Q. Xu, H.J. Sun, R.X. Xu, Dielectric and piezoelectric properties of lead-free $(Na_{0.5}Bi_{0.5})TiO_3$–$NaNbO_3$ ceramics, Mater. Sci. Eng. B 112 (2004) 5–9.

[23] Y. Hiruma, Y. Imai, Y. Watanabe, H. Nagata, T. Takenaka, Large electrostrain near the phase transition temperature of $(Bi_{0.5}Na_{0.5})TiO_3$–$SrTiO_3$ ferroelectric ceramics, Appl. Phys. Lett. 92 (2008) (262904-3).

[24] A.B. Kounga, S Zhang, W. Jo, T. Granzow, J. Rödel, Morphotropic phase boundary in $(1-x)Bi_{0.5}Na_{0.5}TiO_3$–$xK_{0.5}Na_{0.5}NbO_3$ lead-free piezoceramics, Appl. Phys. Lett. 92 (2008) 222902–222903.

[25] X. Zheng, G. Zheng, Z. Lin, Z. Jiang, Electro-caloric behaviors of lead-free $Bi_{0.5}Na_{0.5}TiO_3$–$BaTiO_3$ ceramics, J. Electroceram. 28 (2012) 20–26.

[26] Y. Kazushige, Y. Hiruma, H. Nagata, T. Takenaka, Electrical properties and depolarization temperature of $(Bi_{1/2}Na_{1/2})TiO_3$-$(Bi_{1/2}K_{1/2})TiO_3$ lead-free piezoelectric ceramics, Jpn. J. Appl. Phys. 45 (2006) 4493–4496.

[27] S. Zhang, A.B. Kounga, E. Aulbach, H. Ehrenberg, Giant strain in lead-free piezoceramics $Bi_{0.5}Na_{0.5}TiO_3$–$BaTiO_3$–$K_{0.5}Na_{0.5}NbO_3$ system, Appl. Phys. Lett. 91 (2007) (112906-3).

[28] Y. Guo, M. Gu, H. Luo, Y. Liu, Composition-induced antiferroelectric phase and giant strain in lead-free $(Na_y,Bi_z)Ti_{1-x}O_{3(1-x)}$-$x$BaTiO$_3$ ceramics, Phys. Rev. B 83 (2011) (054118-7).

[29] V. Dorcet, G. Trolliard, A transmission electron microscopy study of the A-site disordered perovskite $Na_{0.5}Bi_{0.5}TiO_3$, Acta Mater. 56 (2008) 1753–1761.

[30] B.N. Rao, A.N. Fitch, R. Ranjan, Ferroelectric–ferroelectric phase coexistence in $Na_{1/2}Bi_{1/2}TiO_3$, Phys. Rev. B 87 (2013) (060102(R)-5).

[31] W. Jo, S. Schaab, E. Sapper, L.A. Schmitt, H.J. Kleebe, A.J. Bell, J. Rodel, On the phase identity and its thermal evolution of lead free $(Bi_{1/2}Na_{1/2})TiO_3$–6 mol% $BaTiO_3$, J. Appl. Phys. 110 (2011) 074106–074109.

[32] G. Viola, H. Ning, M.J. Reece, R. Wilson, T.M. Correia, P. Weaver, M. G. Cain, H. Yan, Reversibility in electric field-induced transitions and energy storage properties of bismuth-based perovskite ceramics, J. Phys. D: Appl. Phys. 45 (2012) 355302.

[33] W. Jo, J. Daniels, D. Damjanovic, W. Kleemann, J. Rödel, Two-stage processes of electrically induced-ferroelectric to relaxor transition in 0.94 $(Bi_{1/2}Na_{1/2})TiO_3$–0.06$BaTiO_3$, Appl. Phys. Lett. 102 (2013) 192903–192904.

[34] G.A. Samara, Ferroelectricity revisited—advances in materials and physics, Solid State Phys. 56 (2001) 239–458.

[35] Y. Dai, S. Zhang, T. Shrout, X. Zhang, Piezoelectric and ferroelectric properties of Li-doped $(Bi_{0.5}Na_{0.5})TiO_3$–$(Bi_{0.5}K_{0.5})TiO_3$–$BaTiO_3$ lead-Free piezoelectric ceramics, J. Am. Ceram. Soc. 93 (2010) 1108–1113.

[36] V. Dorcet, G. Trolliard, P. Boullay, Reinvestigation of phase transitions in Na0.5Bi0.5TiO3 by TEM. part I: first order rhombohedral to orthorhombic phase transition, Chem. Mater. 20 (2008) 5061–5073.

[37] J.E. Daneils, W. Jo, J. Rödel, V. Honkimäkia, J.L. Jones, Electric-field-induced phase-change behavior in $(Bi_{0.5}Na_{0.5})TiO_3$–$BaTiO_3$–$(K_{0.5}Na_{0.5})NbO_3$: a combinatorial investigation, Acta Mater. 58 (2010) 2103–2111.

[38] W. Ge, D. Maurya, J. Li, S. Priya, D. Viehland, Alternating and direct current field effects on the structure-property relationships in $Na_{0.5}Bi_{0.5}$-TiO_3–x%$BaTiO_3$ textured ceramics, Appl. Phys. Lett. 102 (2013) 222905 (–5).

[39] A.-K. Axelsson, F Le Goupil, L.J. Dunne, G. Manos, M Valant, N. McN., Alford, Microscopic interpretation of sign reversal in the electrocaloric effect in a ferroelectric $PbMg_{1/3}Nb_{2/3}O_3$–$30PbTiO_3$ single crystal, Appl. Phys. Lett. 102 (2013) 102902–102904.

[40] I. Ponomareva, S. Lisenkov, Bridging the macroscopic and atomistic descriptions of the electrocaloric effect, Phys. Rev. Lett. 108 (2012) 167604–167605.

[41] Y. Bai, X. Han, L. Qiao, Optimized electrocaloric refrigeration capacity in lead-free $(1-x)BaZr_{0.2}Ti_{0.8}O_3$–$xBa_{0.7}Ca_{0.3}TiO_3$ ceramics, Appl. Phys. Lett. 102 (2013) 252904 (–4).